In all tests, the compression tube was initially filled with air at 1 atm, and a piston driver reservoir pressure of 40 atm was used. A test was initiated by releasing the piston from the launcher, whereupon it was driven rapidly along the compression tube, compressing the air in the tube until it reached a pressure such that the primary diaphragm ruptured. This diaphragm, which was made of mild steel, ruptured under static hydraulic tests at a pressure of 250 atm. Taking this as the rupture pressure under the conditions of the experiments, and assuming isentropic compression of the driver gas in the compression tube, it follows that the temperature of driver gas at rupture was 1400°K. Rupture of the primary diaphragm caused a shock wave to traverse the intermediate shock tube and reflect from the secondary diaphragm. This was made of aluminium, 1.27 mm thick, and was scribed to a depth of approximately 0.35 mm. Upon reflection of the shock wave this diaphragm would begin to yield. The process of yield prior to opening of the diaphragm was of time duration sufficient to allow formation of a quiescent slug of shock heated air adjacent to the diaphragm, and this acted as the driver gas for the test shock tube.

Shock speeds in the test shock tube were measured using three piezoelectric pressure transducers, which were manufactured in the laboratory and mounted with careful attention to requirements of vibration isolation. The transducers were located as shown in Fig. 1b, and their output was displayed on a Solarton CD1400 C.R.O., with precalibrated sweep. Initial shock tube pressures were read using a mercury manometer, with a micrometer screw reading attachment. The optimum initial pressure in the intermediate tube was determined by performing a series of tests with an initial pressure of 1 torr in the test shock tube, It was found that maximum shock speeds were achieved with an intermediate tube pressure of 0.56 atm, and this was used in all subsequent tests.

Shock speeds in the test shock tube were measured over a range of initial tube pressures. Results obtained for the shock speed between the two downstream timing stations are displayed in Fig. 2, where it can be seen that shock Mach numbers of 13 have been achieved. Shock attenuation varied with shock speed. For example, at $M_S = 6$ the shock decelerated by approximately 8%/m, at $M_S = 10$ no change in speed was observed, and at $M_S = 13$ the shock accelerated by approximately 5%/m.

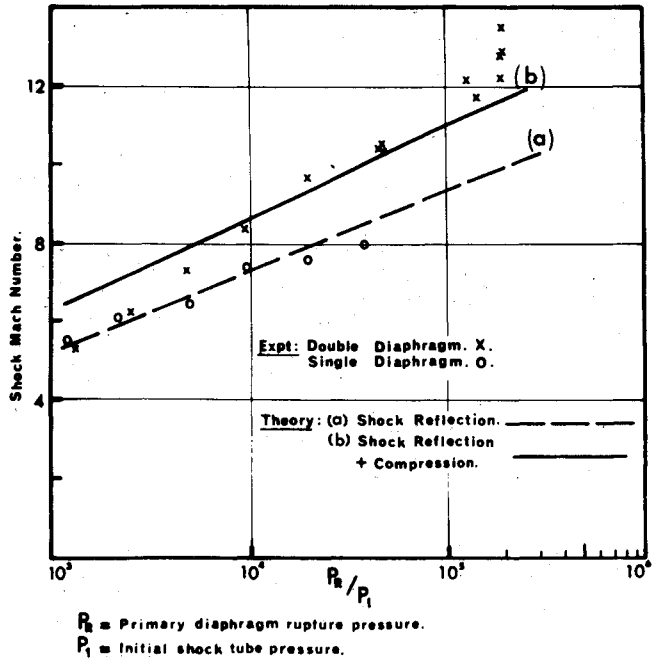

Fig. 2 Measured shock speeds in air.

The benefit conferred through use of the secondary diaphragm is illustrated in Fig. 2., by comparing the shock speeds plotted with those obtained in the absence of this diaphragm. It can be seen that at high shock speeds a gain exceeding 30% was achieved. Using the initial intermediate tube pressure employed in the tests, and shock speeds measured without the secondary diaphragm, it was calculated that a pressure of 79 atm and an ideal gas temperature of 2700°K would be reached in shock reflection from the secondary diaphragm. Assuming ideal gas behavior in the subsequent unsteady expansion of the shock heated gas, the shock speeds indicated by the theoretical curve (a), in Fig. 2, were obtained. These underestimate the measured values. However, calculations which were made by allowing isentropic compression to twice the shock reflection pressure before subsequent unsteady expansion in the shock tube produced the curve (b) in Fig. 2. Noting that the shock wave decelerated at low speeds, and accelerated at high speeds, it is clear that curve (b) provides reasonable estimates of the mean value of the shock speed over the length of the shock tube. Thus, the results suggest that compression subsequent to shock reflection in the gas in the intermediate tube plays a role in producing the high shock speeds measured.

The experiments reported show that strong shock waves can be produced with safety and economy by using a free piston shock tube with air as driver gas.

References

[1] Copper, J. A., Miller, H. R., and Hameetman, F. J., "Correlation of Uncontaminated Test Durations in Shock Tunnels," *Proceedings of the Fourth Hypervelocity Techniques Symposium*, Univ. of Denver, Denver, Colo., 1964, pp. 274–310.

[2] Stalker, R. J., "The Free-Piston Shock Tube," *Aeronautical Quarterly*, Vol. 17, Pt. 4, Nov. 1966, pp. 351–370.

[3] Stalker, R. J. and Plumb, D. L., "Diaphragm-Type Shock Tube for High Shock Speeds," *Nature*, Vol. 218, May 1968, pp. 789–790.

A New Assumed Stress Hybrid Finite Element Model for Solid Continua

SATYANADHAM ATLURI*
University of Washington, Seattle, Wash.

Introduction

IT is comparatively recent that several finite element models were formulated from different variational principles of solid mechanics, and their modifications, by systematically relaxing the continuity requirements at the interelement boundaries of adjoining discrete elements. A systematic classification of such finite-element methods is given by Pian and Tong,[1] and the author.[2] The commonly used assumed displacement models satisfy the requirements of interelement displacement field continuity and the rigid-body mode representation to various degrees; however, the strain and stress fields are discontinuous across the interelement boundaries. Tong[3] constructed a finite-element model, wherein an arbitrary smooth displacement field is assumed in the interior, and the interelement displacement compatibility is satisfied in the average by prescribing an independent compatible element-boundary displacement field and choosing an arbitrary set of boundary tractions as Lagrangian multipliers. In this

Received March 22, 1971. The author wishes to thank J. Fuchs who provided the motivation.

* Assistant Professor, Department of Aeronautics and Astronautics.

model also, the strain and stress fields are discontinuous at element boundaries. Also, in the displacement model finite-element analysis, it is, in general, difficult to satisfy the stress-free conditions at the boundaries of the solid. With the assumed stress formulation, one can construct a direct analog of the compatible displacement model, with the analogy between the stress functions (the so-called static-geometric analogy, especially in linear shell theory) and displacement functions being maintained, and the unknowns in the final set of finite-element equations as the nodal values of stress functions. In this formulation, even though the stress functions may be continuous across the interelement boundaries, the stresses, in general, are not; also, it is a difficult task to include prescribed body forces and the physical interpretation of the boundary conditions for the stress functions is often obscure. There are two other assumed stress finite element models, in both of which the unknowns in the final set of equations are the nodal generalized displacements; one is an equilibrium model developed by Fraeijis de Veubeke and Sander[4] and the other is a hybrid model developed by Pian.[5] In the equilibrium model, an equilibrium stress field that is continuous across the interelement boundaries is assumed for each element, whereas inter-element boundary displacement compatibility is satisfied only in the average. Again, as it is a matrix displacement formulation, it is not easy to satisfy the stress boundary conditions. In Pian's formulation,[5] stress equilibrium in the interior of the element as well as interelement boundary displacement compatibility are satisfied, and the inter-element stress continuity is satisfied only in an average. Though in principle one can a priori choose the parameters in the stress field of each individual element to satisfy the relevant stress boundary conditions, it is nevertheless complicated in practice. As Pian's formulation is also a matrix displacement formulation it is difficult to satisfy the stress boundary conditions in a routine way. There exists a class of problems, such as the analysis of the stress states around holes, cut-outs, and around extending cracks in fracture mechanics[6] in which the stress boundary conditions (or stress-free conditions) have to be satisfied exactly. The principal purpose of this note is to present a convenient way of handling such problems.

Assumed Stress Hybrid Element Formulation

In what follows, for simplicity, only Cartesian tensors are used. It has already been shown by Hu[7] and Washizu[8] that the functional, in linear elasticity,

$$\pi = -\int_V \{[\sigma_{ij}\epsilon_{ij} - A(\epsilon_{ij})] + (\sigma_{ij,j} + \bar{X}_i)u_i\}dV + \int_{S_1}(T_i - \bar{T}_i)u_i dS + \int_{S_2} T_i\bar{u}_i dS \quad (1)$$

in which σ_{ij} is the stress tensor, ϵ_{ij} is the strain tensor, A is the strain-energy functional, $\bar{X}_i$ are prescribed body forces, V is the volume of the body, S_1 is the boundary of the body where tractions are prescribed, $\bar{T}_i$ are the prescribed boundary tractions, T_i are the internal tractions at the boundary, S_2 is the boundary of the body where displacements are prescribed, $\bar{u}_i$ are the prescribed boundary displacements, and a comma denotes a differentiation; has the variational equation

$$\delta\pi = \int_V \{(\partial A/\partial\epsilon_{ij} - \sigma_{ij})\delta\epsilon_{ij} - [\epsilon_{ij} - \tfrac{1}{2}(u_{i,j} + u_{j,i})]\delta\sigma_{ij} - (\sigma_{ij,j} + \bar{X}_i)\delta u_i\}dV + \int_{S_1}(T_i - \bar{T}_i)\delta u_i - \int_{S_2}(u_i - \bar{u}_i)\delta T_i dS = 0 \quad (2)$$

The corresponding Euler equations of Eq. (2) can be written as

$$\sigma_{ij} = \partial A/\partial\epsilon_{ij}; \quad \epsilon_{ij} = \tfrac{1}{2}(\partial u_i/\partial x_j + \partial u_j/\partial x_i)$$
$$\sigma_{ij,j} + \bar{X}_i = 0 \text{ in } V;$$
$$T_i = \bar{T}_i \text{ in } S_1; \quad \text{and} \quad u_i = \bar{u}_i \text{ in } S_2. \quad (3)$$

If one assumes a priori that $\sigma_{ij} = \partial A/\partial\epsilon_{ij}$, and $\sigma_{ij,j} + \bar{X}_i = 0$ in V, then the functional in Eq. (1) can be modified as,

$$-\pi_F = -\int_V B dV + \int_{S_1}(T_i - \bar{T}_i)u_i dS + \int_{S_2} T_i\bar{u}_i dS \quad (4)$$

where B is the stress-energy functional (strain-potential).

The functional in Eq. (4) can be evaluated for each discrete element of a finite-element assembly and can then be summed over the number of elements to find the functional for the assembly. Thus, one can assume an arbitrary equilibrating stress field, in the interior of each element, that need not satisfy continuity at the element boundaries, and then enforce inter-element continuity of stresses using a Lagrangian multiplier technique. Thus, for a finite-element assembly, one can write,

$$-\pi_F = \Sigma_m \{-\int_{V_m} B dV + \int_{\delta V_m}(T_i - \bar{T}_i)u_{iL}\delta V_m + \int_{S_{u_m}} T_i\bar{u}_i\} \quad (5)$$

in which the following interpretation can be given: m is the number of elements, V_m is the volume of the mth element, δV_m is the boundary of the mth element, T_i are the boundary tractions generated by the assumed stress field in the interior of the mth element, $\bar{T}_i$ are the independently prescribed tractions, at the boundary of the mth element, that are inherently compatible with those of the neighboring elements, u_{Li} are the Lagrangian multiplier terms which can be interpreted as the boundary displacements, S_{um} is the portion of the boundary of the mth element where displacements $\bar{u}_i$, if any, are prescribed. Noting that the increments of stress satisfy the equation $\delta\sigma_{ij,j} = 0$, it can be shown that the variation of the functional in Eq. (5) is

$$\delta\pi_F = \Sigma_m \{-\int_{V_m}[\epsilon_{ij} - \tfrac{1}{2}(u_{i,j} + u_{j,i})]\delta\sigma_{ij}dV + \int_{\partial V_m}(T_i - \bar{T}_i)\delta u_{iL}dS + \int_{\partial V_m}(u_{iL} - u_i)\delta T_i dS + \int_{S_{u_m}}\delta T_i(\bar{u}_i - u_i)dS\} = 0 \quad (6)$$

Since $\delta\sigma_{ij}$, δu_{iL}, and δT_i are arbitrary and independent for each element, the Euler equations corresponding to Eq. (6) can be written as,

$$\epsilon_{ij} = \tfrac{1}{2}(u_{i,j} + u_{j,i}) \quad \text{in} \quad V_m; \quad T_i = \bar{T}_i \quad \text{on} \quad \partial V_m$$
$$u_{iL} = u_i \quad \text{on} \quad \partial V_m; \quad \text{and} \quad u_i = \bar{u}_i \quad \text{on} \quad S_{um} \quad (7)$$

Thus, in the finite-element analysis, for each individual element, one assumes the following.

1) An element interior stress field as

$$\{\sigma_{ij}\} = [R]\{\alpha\} + \{R_2\} \quad (8)$$

where $\{\alpha\}$ is a column of undetermined parameters, $[R]$ a set of functions (polynomials, for instance) representing a self-equilibrating solution, and $\{R_2\}$ any particular solution that is statically equivalent to the applied body forces.

2) An independently prescribed element boundary traction as

$$\{\bar{T}_i\} = [\Phi]\{Q\} \quad (9)$$

where $\{Q\}$ are the generalized forces at a finite number of nodal points along the boundary and the matrix of functions $[\Phi]$ is so chosen that the tractions along the boundary are uniquely interpolated in terms of their respective nodal values, $\{Q\}$. Since the $\{Q\}$'s are the same for any two neighboring elements sharing a common boundary, interelement boundary traction continuity is inherently satisfied.

3) A set of Lagrangian multiplier terms u_{iL} (physically interpreted as displacements) at the element boundary as

$$\{u_{iL}\} = [U]\{\beta\} \quad (10)$$

where $\{\beta\}$ are the undetermined parameters and $[U]$ is an arbitrary set of functions.

Substituting Eqs. (8–10) in Eq. (5), one can write

$$-\pi_F = \Sigma_m(-\tfrac{1}{2}\lfloor\alpha\rfloor[H]\{\alpha\} - \lfloor\alpha\rfloor\{F_1\} + \lfloor\alpha\rfloor[P]\{\beta\} + \lfloor\beta\rfloor\{F_2\} - \lfloor\beta\rfloor[G]\{Q\} + C_m) \quad (11)$$

where

$$[H] = \int_{V_m} [R]^T[C][R]dV \tag{12}$$

$$\{F_1\} = 2\int_{V_m} [R]^T[C]\{R_2\}dV + \int_{S_{u_m}} T_i\bar{u}_i$$

$$\lfloor \alpha \rfloor[P]\{\beta\} + \lfloor \beta \rfloor\{F_2\} = \int_{\partial V_m} \lfloor T_i \rfloor\{u_{Li}\}dS \tag{13}$$

$$\lfloor \beta \rfloor[G]\{Q\} = \int_{\partial V_m} \lfloor u_{Li} \rfloor\{\bar{T}_i\}dS \tag{14}$$

and C_m is a constant. In the above $[C]$ is the elasticity compliance matrix. Since only the parameters $\{\alpha\}$ and $\{\beta\}$ are independent for each element, taking the variation of Eq. (1) with respect to $\{\alpha\}$ and $\{\beta\}$, leads to the Euler equations for each element, as

$$-[H]\{\alpha\} - \{F_1\} + [P]\{\beta\} = 0 \tag{15}$$

and

$$[P]^T\{\alpha\} + \{F_2\} - [G]\{Q\} = 0 \tag{16}$$

From Eqs. (15) and (16) one can solve for $\{\alpha\}$ and $\{\beta\}$ as,

$$\{\alpha\} = +[H]^{-1}[P]\{\beta\} - [H]^{-1}\{F_1\} \tag{17}$$

and

$$\{\beta\} = ([P]^T[H]^{-1}[P])^{-1}[G]\{Q\} + ([P]^T[H]^{-1}[P])^{-1}([P]^T[H]^{-1}\{F_1\} - \{F_2\}) \tag{18}$$

It can be seen from the above equations that the number of α's must be larger or equal to the number of β's and the rank of $[P]$ equal to the number of β's in order to have $\{\beta\}$ and $\{\alpha\}$ solvable in terms of $\{Q\}$. Substituting Eqs. (17) and (18) in Eq. (11), one can express π_F in terms of $\{Q\}$ alone, as,

$$\pi_F = +\Sigma_m (+\tfrac{1}{2}Q[D_m]\{Q\} - Q\{E_m\} + C_m^*) \tag{19}$$

where

$$[D_m] = [G]^T([P]^T[H]^{-1}[P])^{-1T}[G] \tag{20}$$

$$\{E_m\} = [G]^T([P]^T[H]^{-1}[P])^{-1T} \times (-[P]^T[H]^{-1}\{F_1\} + \{F_2\}) \tag{21}$$

The matrix $[D_m]$ is symmetric and positive definite because $[H]$ is symmetric and positive definite and the rank of $[P]$ is equal to the number of β's. Using the generalized nodal forces $\{Q^*\}$ for the finite-element assembly, and since these can be subjected to independent variation, one obtains a final set of equations of the form

$$[D]\{Q^*\} = [E] \tag{22}$$

In Eqs. (20) and (21), in order to form $[D_m]$ and $[E_m]$, matrix inversions have to be performed twice. But, if there are as many β's as α's, it can be seen from Eq. (13) that the matrix $[P]$ becomes square. Hence,

$$(P^TH^{-1}P)^{-1} = [P]^{-1}[H][P^T]^{-1} \tag{23}$$

Thus, the expressions for $[D_m]$ and $[E_m]$ can be simplified as

$$[D_m] = [G]^T[P^{-1}][H][P]^{-1T}[G] \tag{24}$$

and

$$\{E_m\} = -G^T[P^{-1}]^T\{F_1\} + [G]^T[P]^{-1}[H][P]^{-1T}\{F_2\} \tag{25}$$

Closure

Unlike in the equilibrium stress model of de Veubeke and Sander,[4] and the hybrid stress model of Pian,[5] the unknowns in the final set of matrix equations for the finite-element assembly in the present assumed stress model are the nodal values of stresses. Thus, stress boundary conditions can be handled more conveniently. This is of advantage in problems such as analysis of stress-states around holes in plane-stress problems, stress-states around cut-outs in shells, and stress-states in plates with extending cracks, where stress-free boundary conditions have to be satisfied. Also, since the stress-states at node points are directly solved for, it is very convenient to apply the yield criteria and flow rules in plasticity problems. The use of the method in such problems is currently being investigated. It should be pointed out that this method is a direct analogy of the hybrid displacement model used by Tong,[3] and the author.[2]

References

[1] Pian, T. H. H. and Tong, P., "Basis of Finite Element Methods for Solid Continua," *International Journal of Numerical Methods in Engineering*, Vol. 1, 1969, pp. 3–28.

[2] Atluri, S., "Static Analysis of Shells of Revolution Using Doubly-Curved Quadrilateral Elements Derived From Alternate Variational Models," SAMSO TR 69-394, June 1969, Norton Air Force Base, Calif., pp. 27–76.

[3] Tong, P., "New Displacement Hybrid Finite Element for Solid Continua," *International Journal of Numerical Methods in Engineering*, Vol. 2, 1970, pp. 73–83.

[4] Fraejis de Veubeke and Sander, G., "An Equilibrium Model for Plate Bending," *International Journal of Solids and Structures*, Vol. 4, 1968, pp. 447–468.

[5] Pian, T. H. H., "Element Stiffness Matrices for Boundary Compatibility and for Prescribed Boundary Stresses," *Proceedings of the Conference on Matrix Methods in Structural Mechanics*, AFFDL TR-66-80, 1965, pp. 457–477.

[6] Kobayashi, A. R., Chiu, S. T. and Beeukes, R., "Elastic-Plastic State in a Plate with an Extended Crack," *Proceedings of the 1970 U.S. Army Conference on Solid Mechanics-Light Weight Structures*, to be published.

[7] Hu, H. C., "On Some Variational Principles in the Theory of Elasticity and Plasticity," *Scintia Sinica*, Vol. 4, No. 1, March 1955, pp. 33–54.

[8] Washizu, K., *Variational Methods in Elasticity and Plasticity*, Pergamon, New York, 1968, pp. 27–51.

An Effective Approximation for Computing the Three-Dimensional Laminar Boundary-Layer Flows

KENNETH K. WANG*

McDonnell Douglas Astronautics Company, Huntington Beach, Calif.

Nomenclature

c	=	density-viscosity ratio, $\rho\mu/\rho_w\mu_w$
f	=	$\int_o^\eta Fd\eta$
F	=	u/u_e
g	=	$\int_o^\eta Gd\eta$
G	=	v/u_e
H	=	total enthalpy
K_1	=	curvature, streamwise
K_2	=	curvature, orthogonal to streamline
Pr	=	Prandtl number
S_1,S_2,S_3	=	curvilinear coordinates in the stream wise, crossflow and normal directions
u,w,v	=	velocity components in the S_1,S_2, and S_3 directions
ρ	=	density
μ	=	viscosity
ξ,ζ,η	=	transformed coordinates

Received October 16, 1970; revision received April 29, 1971. This work was supported by the McDonnell Douglas Astronautics Company Independent Research and Development (IRAD) program.

Index Category: Boundary Layers and Convective Heat Transfer—Laminar.

* Senior Engineer/Scientist, Aero/Thermodynamics and Nuclear Effects Department.